

Numerical Simulation of 3-D One-Way Fluid-Structure Interaction in a Tube with Twisted Tape under Laminar and Turbulent Flow Regime

Laith J. Habeeb¹, Fouad A. Saleh², Bassim M. Maajel²

¹Mechanical Engineering Department, University of Technology, Baghdad, Iraq.

²Mechanical Engineering Department, University of Almustansiriyah, Baghdad, Iraq.

Abstract

Fluid-structure interaction (FSI) analysis is an example of a multi-physics problem where the interaction between two different analyses is taken into account. The FSI analysis involves performing a structure analysis taking into account the interaction with the corresponding fluid analysis. The interaction between the two analysis typically takes place at the boundary of the model solution (the fluid-structure interface), where the results of one analysis is passed to the other analysis as a load. The Fluid-Structure Interaction has gained great interest of scholars recently, meanwhile, extensive studies have been conducted by the virtue of numerical methods which have been implemented on heat exchanger models. This paper presents numerical results of the fluid-structure investigation in a circular finned-tube heat exchanger. Results are obtained with the use of ANSYS-15 commercial code. Simulation is conducted in the Reynolds number range of (1009–10172) with tape of twist ratio ($H/D = 1.85$). In this study, the effect of total deformation of structure, strain and stress for the tube and twisted tape are observed. We performed the one-way FSI analysis on a finned-tube, using the Finite Volume Method with ANSYS-fluent solver and the RNG k- ϵ turbulence model for turbulent flow, to achieve a comprehensive cognition of it. The simulation results show that the maximum deformation occurs in the area before the end of the tape due to high temperature with a maximum stress of (1 MPa and 1.3 MPa) for laminar and turbulent flow respectively. This study highlights that a one-way fluid structure interaction simulation of a real engineering configuration is still a challenging task for today's commercially available simulation tools.

Keywords: Fluid-structure interaction, RNG k- ϵ turbulence model, Finned-tube, One-Way Fluid-Structure.

INTRODUCTION

Fluid-structure interaction (FSI) problems are of special interest for engineers and designers in a wide range of industrial areas including hydrodynamics, aerodynamics, civil engineering, and biomechanics. Yet a comprehensive study of such problems remains a challenge due to their strong nonlinearity and multidisciplinary nature. For most FSI problems, analytical solutions to the model equations are impossible to obtain, whereas laboratory experiments are limited in scope; thus to investigate the fundamental physics involved in the complex interaction between fluids and solids,

numerical simulations may be employed. The investigation of fluid-structure interaction as in the form known to engineers working in the area of pressure vessels and piping systems is considered to have begun in the 1960s.

In 1966, Fritz and Kiss performed a study on the vibration response of a cantilever cylinder surrounded by an annular fluid, which is known to be the pioneering study of fluid-structure interaction for power plants. From the early 1970s to the late 1980s, a lot of investigators studied the dynamics of interaction between fluid and elastic shell systems including pipes, tubes, vessels, and co-axial cylinders. In fact the history of fluid-structure interaction has been previously reported by Au-Yang, M.K. (2001). The objectives of fluid structure interaction has comparatively been less acclaimed in literature therefore the number of the publications dealing with it is limited. The most productive research has been continuously carried out by the following studies:

Huang et al. [1] studied the natural frequency of fluid structure interaction in a pipeline conveying fluid in different boundary conditions, by using the eliminated element-Galerkin method. The natural frequency of a straight pipe simply supported at both ends was calculated taking into account the Coriolis force. The four components (i.e. mass, stiffness, length and flow velocity) were studied in detail. The flow velocity relates to the natural frequency. The results indicated that the effect of Coriolis force on the natural frequency was inappreciable.

Bettinali et al. [2] studied the effect of earthquake motion along the axial length of a single pipe. They described the development of a coupled FSI model that includes liquid column separation and Poisson coupling. A calculation of a postulated seismic load on the pipe showed that coupled analysis predicts lower pressure amplitudes than uncoupled analysis.

Sreejith et al. [3] introduced a finite element formulation to the fully coupled dynamic equations of motion to include the effect of FSI, and it can be applied to a pipeline system used in nuclear reactors. The wave equation is formulated in terms of velocity. The finite element formulation is first verified through a valve closure excitation experiment for a simple pipeline geometry. The formulation was then applied to a secondary sodium pipeline of a fast breeder reactor to determine the effect of FSI on structural velocities. Numerical studies shows that structural velocities reduce significantly if FSI effects are considered in the analysis of fluid filled

pipelines subjected to fluid transients like valve closure excitation.

Hatfield and Wiggert [4] conducted a numerical study in which an aboveground 3D pipe system was subjected to simulated earthquake ground motion; the motion was directed to excite the fundamental mode of the piping. The piping was filled with non-moving liquid, and component synthesis was used assuming no Poisson coupling. It was found that allowing the piping to be rigid produced an upper bound estimate of pressure, and conversely, assuming the liquid to be incompressible resulted in underestimating displacement of the piping.

Moussou et al [5] analyzed Z-shaped piping that contained two vibrating elbows using both a 3D and a simplified 1D numerical code. They compared two piping / fluid models: one where the mass of the fluid is added to the mass of the pipe wall and the other a fully coupled FSI model. The correct latter approach leads to a description of the coupled modes of vibration and the development of a transfer function relating the structural displacement to the applied pressure perturbation.

Fan et al. [6] investigated numerically and experimentally the simultaneous occurrence of fluid-structure interaction (FSI) and vaporous cavitation in the transient vibration of freely suspended horizontal pipe systems. Extended water hammer and beam equations, including the relevant FSI mechanisms, are solved by the method of characteristics. Column separation and cavitation are accounted for by a lumped parameter model. They found Close agreement between numerical results and unique experimental data obtained in a single-elbow pipe system.

Vardy et al. [7] studied experimentally the interactions between stress waves in the pipes and pressure waves in the contained liquid. The apparatus consists of suspended horizontal pipes which are struck externally by a long horizontal rod. Cavitation, external restraints and preexisting pressure gradients are all absent. They demonstrated that coupling at boundaries and, to a lesser extent, coupling at wave fronts propagating along a pipe can have a major influence on stress and pressure histories. They also shown that coupling changes the fundamental frequencies of vibration in comparison with those deduced by considering the liquid and solid components alone.

Tijsseling [8] presented a one-dimensional mathematical model to describe the acoustic behavior of thick-walled liquid-filled pipes. The model is based on conventional water-hammer and beam theories. Fluid-structure interaction (FSI) is taken into account. The equations governing straight pipes are derived by the cross-sectional integration of axisymmetric two-dimensional basic equations. The resulting FSI four equation model has small correction terms and factors accounting for the wall thickness. Exact solutions of this model show that these corrections are important only for very thick pipes, with, say, a radius/thickness ratio smaller than 2.

Berlinsky et al. [9] developed a channel model for the purpose of simulating the interactive fluid-structural response of curved pipes to pressure pulses. Simulation is shown to have

been achieved analytically in both the axisymmetric ("breathing") and transverse ("bending") modes of interactive behavior. They described an experimental program for the validation of the model. Tests were run in both straight and curved pipe configurations. Comparisons between measurements and model calculations demonstrate the validity of the model within the range of parameters under consideration.

This study focuses on the one-way FSI analysis of the finned-tube with typical twisted tape, taking the hydrodynamic pressure and heat loading on the internal surface into consideration.

TECHNICAL DETAILS

Physical Models

The configuration of the finned-tube and typical twisted tape (TT) insert are shown in figures 1 and 2 respectively. Copper tape of 1 mm thickness and 22 mm width is uniformly winding over a length 1.5 m to produce twist ratio of 1.85. The twist ratio "y" is defined as the ratio of the length of one full twist (360°) to the tape width. Aluminum finned-tube with a diameter (D) of 2.2 cm and length (L) of 150 cm is used as test section, water which is assumed to be incompressible fluid and Al₂O₃ nanoparticles (d_p = 20 nm) are selected as the working fluid. The thermophysical properties of fluid and materials used for simulation are shown in tables 1 and 2.

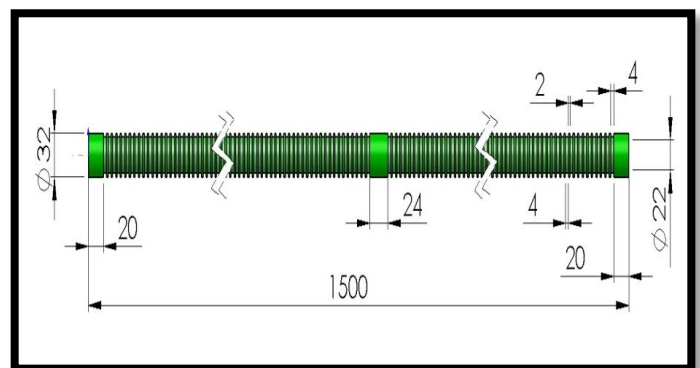


Figure 1: Physical geometry of finned tube.

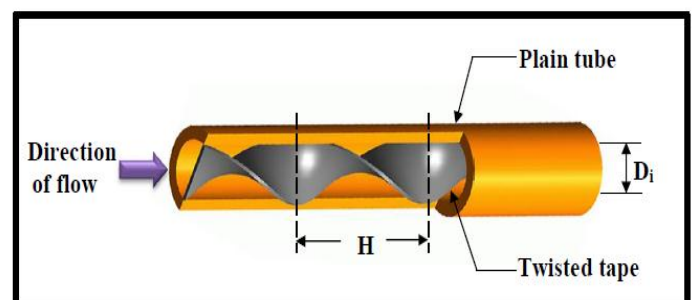


Figure 2: Diagram of a twisted tape insert inside a tube.

Table 1: Properties of nanofluid with different concentration of Al₂O₃.

properties	$\phi = 0 \%$	$\phi = 3 \%$	$\phi = 5 \%$
k_{nf} (W/m.K)	0.600	0.631	0.652
ρ_{nf} (kg/m ³)	998.2	1084.65	1142.29
μ_{nf} (Kg/m.s)	0.001002	0.001332	0.001676
$C_{p,nf}$ (J/kg K)	4182	3816.16	3603.03
k_{nf} / k_{bf}	1	1.051	1.086
μ_{nf} / μ_{bf}	1	1.329	1.672

Table 2: The properties for the nanosized particle at (25 °C).

Particle	Mean diameter (nm)	Density (kg/m ³)	Thermal conductivity (W/m.°C)	Specific heat (J/kg.°C)
Al ₂ O ₃	20	3970	40	765

In one-way interaction, the results (forces) from the fluid analysis at the fluid-structure interface are applied as a load to the structure analysis. The boundary displacement from the structure is not passed back to the fluid analysis. The assumption is that the deformation of the structure is small, having insignificant effect on the fluid flow prediction. This allows the fluid analysis and structure analysis to be run independently. This technique will be used for the theoretical analysis.

Figure (3) explains the one way coupling method. Initially, the fluid flow calculation is performed until convergence is reached. Then the resulting forces at the interface from fluid calculation are interpolated to the structural mesh. After that, the structural dynamic calculations are performed until the convergence criterion is met. This is repeated until the end time is reached.

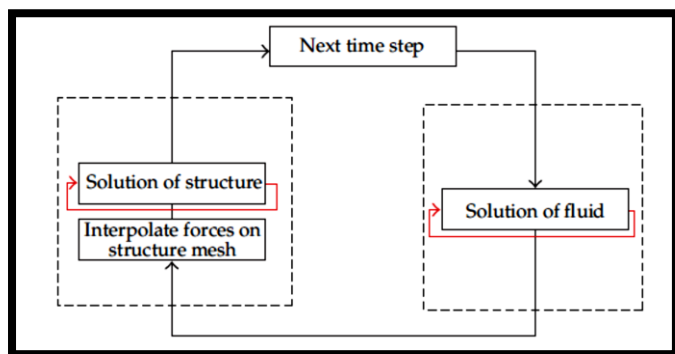


Figure 3: One-way coupling flow chart.

Thermophysical Properties of Nanofluid:

The physical and thermal properties such as density and

specific heat of the nanofluid are calculated using different formulae presented in the literature as outlined below with equations (1) to (4). All properties are calculated using bulk temperatures between inlet and outlet.

$$\rho_{nf} = \left(\frac{m}{V} \right)_{nf} = \frac{\rho_{bf} V_{bf} + \rho_p V_p}{V_{bf} + V_p} = (1 - \phi)\rho_{bf} + \phi\rho_p \dots\dots\dots (1)$$

$$C_{p,nf} = \frac{(1 - \phi)\rho_{bf} C_{p,bf} + \phi\rho_p C_{p,p}}{\rho_{nf}} \dots\dots\dots (2)$$

$$\mu_{nf} = (1 + 7.3\phi + 123\phi^2)\mu_{bf} \dots\dots\dots (3)$$

$$k_{nf} = k_{bf}(1 + 7.74\phi) \dots\dots\dots (4)$$

Where ϕ is the volume concentration and μ is the dynamic viscosity. The index nf, bf and p refers to nanofluid, base fluid and particle properties respectively. In fact there is no reliable data base for viscosity and thermal conductivity of nanofluids and their values can vary significantly depending on the relation used to calculate them.

NUMERICAL PROCEDURE

Geometry Creation with Meshing

Annular-Finned Tube

A circular finned- tube of diameter 22 mm and length 1500 mm was used as the geometry. A 3-D geometry is created by using Ansys Workbench. Unstructured meshing method is used for meshing the geometry. It is meshed into 67,096 nodes and 207,058 elements as shown in figure (4).

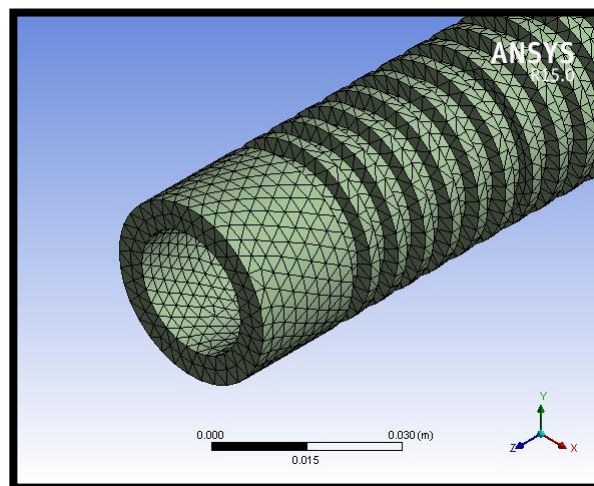


Figure 4: Meshing of plain tube geometry.

Twisted Tape Inserts inside a Finned Tube

The 3D geometry of twisted tape insert inside a finned tube created by using Ansys code 15.0 software and schematic view is shown in the figure (5). The geometry is meshed into smaller cells. The meshing method used is patch independent tetrahedron. The geometry is meshed into 94,892 nodes and 44,044 elements as shown in figure (6).

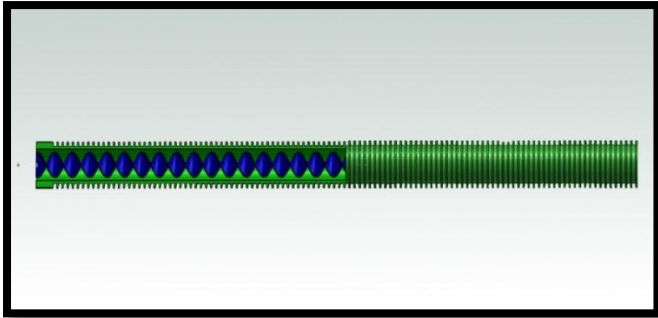


Figure 5: Geometry of twisted tape inside a finned tube.

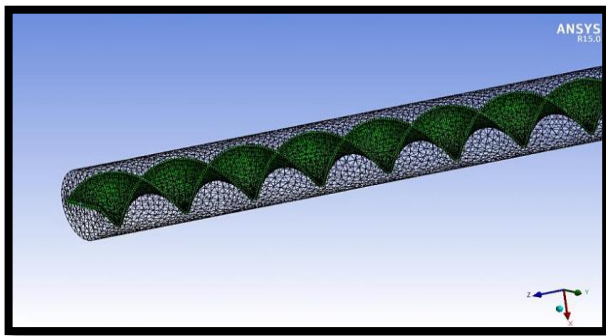


Figure 6: Meshing of twisted tape insert geometry.

Governing Equation

This section provides the detailed information on the governing equations for the CFD and FSI simulation. Commercially available Finite Volume Analysis software, ANSYS 15.0 is used in the present study for CFD and FSI simulation.

Equations for CFD

The solution of the fluid side is based on the continuity equation and the Navier-Stokes equation. The Navier-Stokes equation, written in Einstein summation convention, is given by (5) :

$$\rho \frac{\partial u_i}{\partial t} + \rho \left(\frac{\partial u_i u_j}{\partial x_j} \right) = -\frac{\partial p}{\partial x_i} + \eta \frac{\partial}{\partial x_j} \left(\frac{\partial u_i}{\partial x_j} + \frac{\partial u_j}{\partial x_i} - \frac{2}{3} \frac{\partial u_k}{\partial x_k} \delta_{ij} \right) \dots\dots\dots(5)$$

A solution for this equation requires a fine discretization in space and time. To reduce the computational effort, the solution variables are split into a mean value and a fluctuation value, as shown in equation (6):

$$\phi = \bar{\phi} + \phi' \dots\dots\dots(6)$$

By using Reynolds averaging, we obtain (7), the Unsteady-Reynolds-Averaged-Navier-Stokes Equation:

$$\rho \frac{\partial \bar{u}_i}{\partial t} + \rho \left(\frac{\partial \bar{u}_i \bar{u}_j}{\partial x_j} \right) = -\frac{\partial \bar{p}}{\partial x_i} + \eta \frac{\partial}{\partial x_j} \left(\frac{\partial \bar{u}_i}{\partial x_j} + \frac{\partial \bar{u}_j}{\partial x_i} - \frac{2}{3} \frac{\partial \bar{u}_k}{\partial x_k} \delta_{ij} \right) - \rho \left(\frac{\partial}{\partial x_j} \overline{u'_i u'_j} \right) \dots\dots\dots(7)$$

The continuity equation and the Navier-Stokes equations are solved using a finite volume approach. Starting with the continuity equation in integral form (8), three terms must be solved: the first term describes the change in mass in the control volume; the second deals with the mass flux through the control volume boundary; the third describes the change of the control volume throughout mesh deformation:

$$\frac{d}{dt} \int_V \rho \cdot dV + \int_S \rho U_j \cdot dn_j + \int_S \rho W_j \cdot dn_j = 0 \dots\dots\dots(8)$$

Equations of FSI solution:

The calculations for the structure side are based on the impulse conservation (9). It is solved using a finite element approach, where a finite element is chosen for each specific problem:

$$[M]\{\ddot{U}\} + [C]\{\dot{U}\} + [K]\{U\} = \{F\} \dots\dots\dots(9)$$

Boundary Conditions

The following statements are considered in order to reduce computational efforts, time and also to achieve reasonable conclusions from the project.

- The structure is considered to be fixed at both ends to avoid the deformation of symmetrical walls of the CFD model.
- Dynamic mesh: Normally, the CFD meshes are preferred to be built by hexahedral cells. But, the CFD mesh of this project is a hybrid mesh (combination of tetrahedral and prism layers). The reason for not using the hexahedral cells is it's incompatibility with the dynamic mesh which is used in the current version of Ansys-Fluent.
- The effect of gravity and structural damping are not included in the structural model.
- The computational fluid model is created with the side boundaries exactly at the ends of the circular finned tube which reduces a large amount of cells.

At the inlet, the fully developed profiles of velocity and temperature are specified. At the outlet, a pressure-outlet condition is used. A constant inlet temperature (60 °C) is imposed on the tube inlet. On the surfaces of the tube wall and twisted tape, no slip conditions are applied. The single-phase approach for nanofluids is adopted in this numerical study. The base fluid and nanoparticles are assumed to be perfectly mixed and, thus, can be treated as a homogeneous mixture. The flow is steady-state. Moreover, the fluid phase and solid particles are assumed to be in thermal equilibrium and move with the same local velocity.

Numerical Method

The commercial CFD solver Fluent 15.0 was used to perform the simulations, based on finite volume approach to solve the governing equations with a segregated solver. The second-

order upwind scheme was used for discretization of convection terms, energy, and turbulent kinetic and turbulent dissipation energy. This scheme ensures, in general especially for tri, tetrahedral and polyhedral mesh flow domain, satisfactory accuracy, stability and convergence [10]. Ansys Fluent provides the option to choose among five pressure-velocity coupling algorithms: SIMPLE, SIMPLEC, PISO, Coupled, and [for unsteady flows using the non-iterative time advancement scheme (NITA)] Fractional Step (FSM). All the aforementioned schemes, except the “coupled” scheme, are based on the predictor-corrector. For the present cases SIMPLE algorithm was used to resolve the coupling between velocity and pressure fields [11].

The acronym SIMPLE stands for Semi-Implicit Method for Pressure-Linked Equations and is essentially a Gauss and correct procedure for calculation of pressure. In general for this algorithm, the discretization of momentum equation for entire domain under assumption of a known pressure distribution is made and the velocity field for u , v , and w is calculated. Velocity distribution satisfies the continuity equation then the solution is showed, otherwise a new pressure distribution should be proposed and so forth the momentum equation and appropriate corrections for the pressure field can be used in order to achieve this goal.

In the analysis of the present study, one-way coupled FSI simulation is adopted. The solution of such analysis requires separate solvers that to be run in a sequential order with synchronization points to exchange information at the interface. For this purpose, the commercially available solver Ansys 15.0 have been applied as CFD. This solver has different meshing requirements; therefore, different meshes are generated for the fluid field and the solid field. The mesh must not be identical at the interface, but it must consist of the identical geometrical surface. The case simulation is running until a convergence criterion is reached, i.e., the change in the deflection from iteration to iteration is less than a certain value.

The under relaxation factors are also considered to be 0.3 and 0.7 for pressure and momentum, respectively. Also, for all simulations the convergence criteria was of 10^{-3} for continuity and velocity components and 10^{-6} for energy. In order to have exact numerical simulation which covers the problem features, good quality mesh generation is necessary. Because of twisting geometry of the problem, tetrahedral elements are used for meshing the whole field, this is because it has priority in the sophisticated geometries, as shown below in figure (7). In addition, fine meshes were needed for near wall regions, grid independency of the problem defined required mesh size to have acceptable results. For all simulations performed in the present study, converged solutions were considered when the residuals resulting from the iterative process for all governing equations did not change with the iteration progress and the computational error may be ignored, then the iteration manually stopped. For most of the cases, the iterations is around (850-1000).

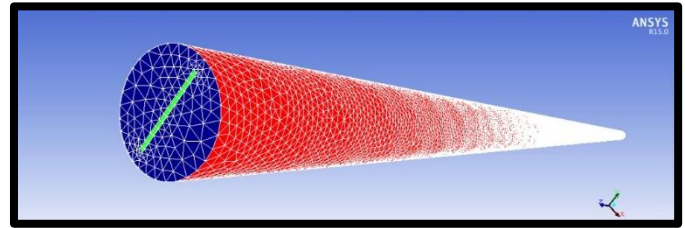


Figure 7: Tetrahedral mesh of the fluid domain with twisted tape.

RESULTS AND DISCUSSIONS

In the one-way interaction, the resulting deformations and stresses are shown and compared below. In order to verify the results of the Fluent- FSI simulation, Ansys-Workbench was used to make sure the results were reasonable.

Total Deformation

Figures (8) to (10) show the deformation of the test section calculated using Static Structural-Mechanical (Ansys WB Module), under the influence enlarge its value (1.8×10^3 Auto Scale). The maximum deformation occurs at the beginning of the tube in all models because high temperature concentration at this region. From these figures, we can see that the total deformation decreases as the volume concentration and mass flow rate increase.

Figure (11) shows the deformation of the twisted tape alone calculated using (Ansys WB Module) for a one-way FSI using Fluent and Static Structural-Mechanical [Ansys Multiphysics] with a maximum deformation calculated to 0.043 mm, under the influence enlarge its value (1.8×10^3 Auto Scale). This figure show that the maximum deflection occurs in the area before the end of the tape, because the tape is fixed from the both sides of the tube, and the thermal effect accumulates at the exit region.

Stress Distribution

Figures (12) and (13) show in true scale the distribution of equivalent von-Mises stress on the test section calculated using Static Structural-Mechanical [Ansys Multiphysics]-Ansys WB Module. The maximum von-Mises stress is (1 MPa) at volume concentration of (5 %) and ($Re = 2033$) for laminar flow. The maximum stress value for turbulent flow is (1.3 MPa) at volume concentration of (5 %) and ($Re = 10172$). It is of importance to note that the maximum von-Mises stress is far from the yield limit which is estimated from material tables to at least 25 MPa. From these figures we can see that the maximum stress occurs in the middle region of the tube.

Strain Distribution

Figure (14) shows in true scale, the distribution of equivalent elastic strain on the test section calculated using Static Structural-Mechanical [Ansys Multiphysics]-Ansys WB Module. The maximum strain is (0.00128 m/m) at volume

concentration of (3 %). From this figure we can see that the greatest strain happens in the central region of the tube.

Modal Analysis

Generally, modal analysis is used to determine the vibrational characteristics of a structure. The vibrational characteristics such as natural frequencies and mode shapes of a structure are important in designing a structure subjected to a dynamic load. It can be considered as a starting point for a transient dynamic analysis. Also, the response of a structure can be evaluated when these modes are excited. The basic equation used in undamped modal analysis is given as:

$$k\phi_i = \omega_n^2 m \phi_i \dots\dots\dots (10)$$

Where: ϕ_i is a mode shape vector (Eigen vector) of mode i , ω_n is a natural frequency of mode i , k is stiffness matrix and m is mass matrix. In fact, the flow wave loads are highly non-linear and time varying and this necessitates the consideration of a dynamic response of twisted tape inside the finned tube and the tube itself. If the period of a wave is close to a natural frequency of a structure and also if the applied load drives the mode shapes then it leads to the resonance and failure of a whole system. So it is an essential process to find out the natural frequencies and its mode shapes of a structure (test section). Generally, the dynamic response of a strip is measured by a parameter called Dynamic Amplification Factor (DAF) which is defined as a ratio of dynamic response amplitude to the corresponding static response.

The result of modal analysis of our case is shown in figure (15). The result includes the first six mode shapes with its respective natural frequency values. There are movies describe the behavior of this made shapes. The first and second modes represent bending in y and z directions respectively. The third and fourth mode shapes show the c -shape in x and y directions respectively. Finally fifth and sixth modes are representing bending in y and s -shape in x directions respectively.

The maximum total deformation occurs in the fourth mode shape, and its value (8.1096 m), but the minimum total deformation occurs in the sixth mode shape, and its value (6.0167 m) as shown in table (3). Table (4) shows list of alternating stress at different cycles for six different mode shapes.

Table 3: List of (ω_n) and total deformation for six different mode shapes.

Mode shapes	Natural frequencies (ω_n) Hz	Total deformation (m)
1	19.024	6.3345
2	20.251	6.4404
3	49.259	7.9924
4	50.559	8.1096
5	51.244	8.0420
6	52.304	6.0167

Table 4: Alternating stress at different cycles for six different mode shapes.

Alternating Stress (Pa)	Cycles	Mean Stress (Pa)
3.999e+009	10	0
2.827e+009	20	0
1.896e+009	50	0
1.413e+009	100	0
1.069e+009	200	0
4.41e+008	2000	0
2.62e+008	10000	0
2.14e+008	20000	0

CONCLUDING REMARKS

This work presented numerical investigation of heat transfer performance and fluid-heat-structure interaction of finned tube with twisted tape inserted. Also, the Al_2O_3 /water as nanofluid is employed in the present heat exchanger. The main concluded points of this study may be summarized as follows:

- 1- In one-way interaction, the total deformation decreases as the volume concentration and mass flow rate increase.
- 2- The maximum deflection occurs in the area before the end of the tape, because the tape is fixed from the both sides of the tube, and the thermal effect accumulates at the exit region.
- 3- The maximum von-Mises stress is (1 MPa) at volume concentration of (5 %) and ($Re = 2033$) for laminar flow, but for turbulent flow is (1.3 MPa) at ($Re = 10172$).
- 4- The maximum strain is (0.00128 m/m) at volume concentration of (3 %).

NOMENCLATURE

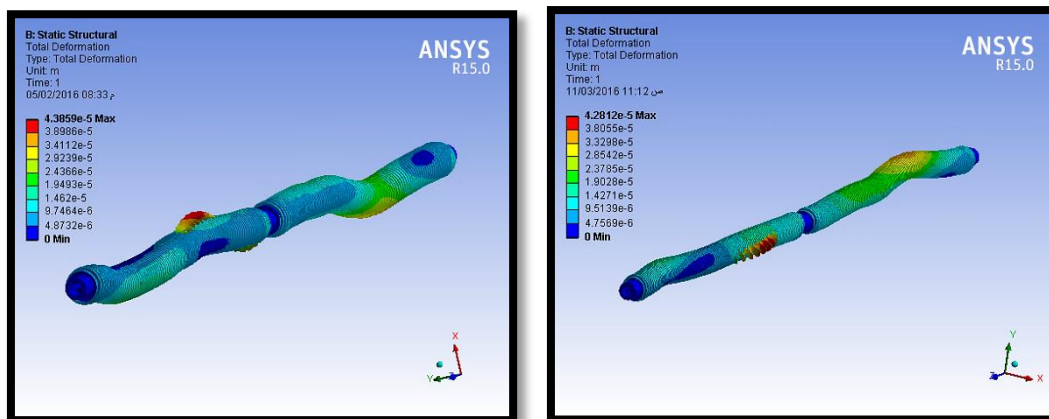
- C_p : Specific heat ($kJ\ kg^{-1}\ ^\circ C^{-1}$)
- D : Tube diameter (m)
- k : Thermal conductivity ($Wm^{-1}\ ^\circ C^{-1}$)
- L : Tube length (m)
- Re: Reynolds number (dimensionless)
- T : Temperature ($^\circ C$)
- TT: twisted tape
- y : Tape ratio

Greek Symbols

- ρ : Density (kgm^{-3})
- ϕ : Nanoparticle volume concentration (dimensionless)

Subscripts

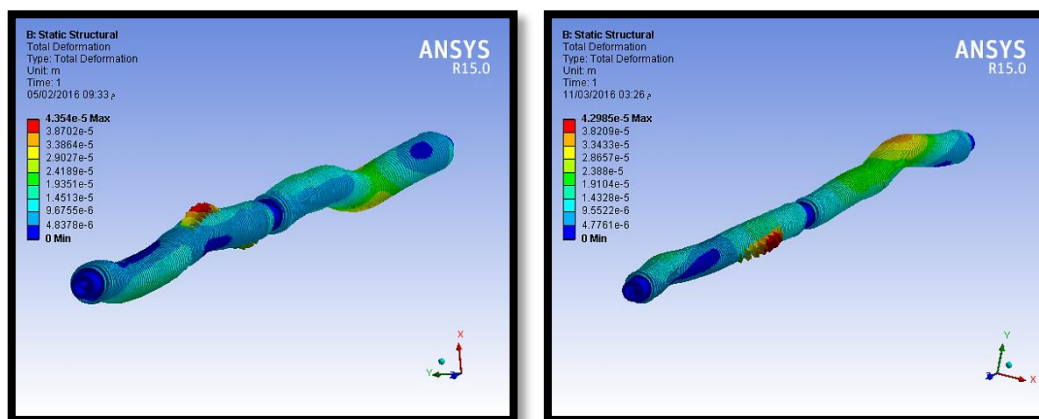
- p : Particles
- bf: Base fluid



$\phi = 0 \%$

$\phi = 3 \%$

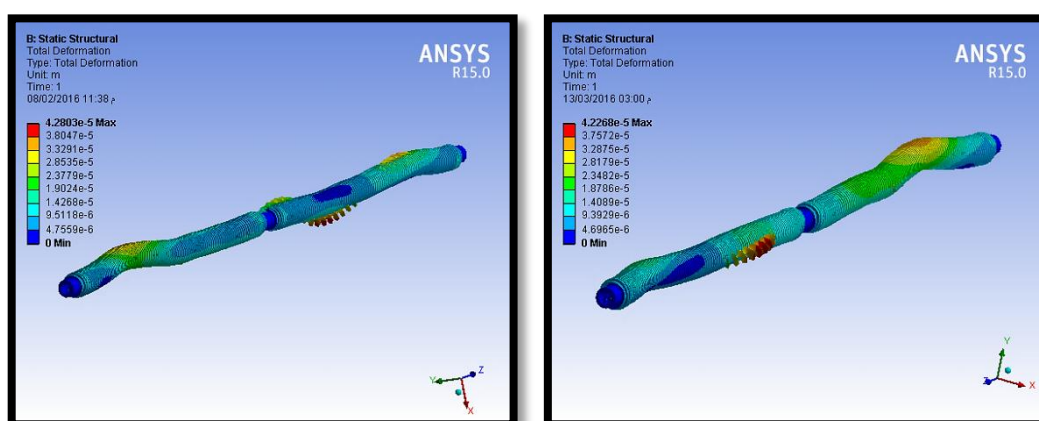
Figure 8: Total deformation from one-way interaction for (Re = 1009).



$\phi = 0 \%$

$\phi = 3 \%$

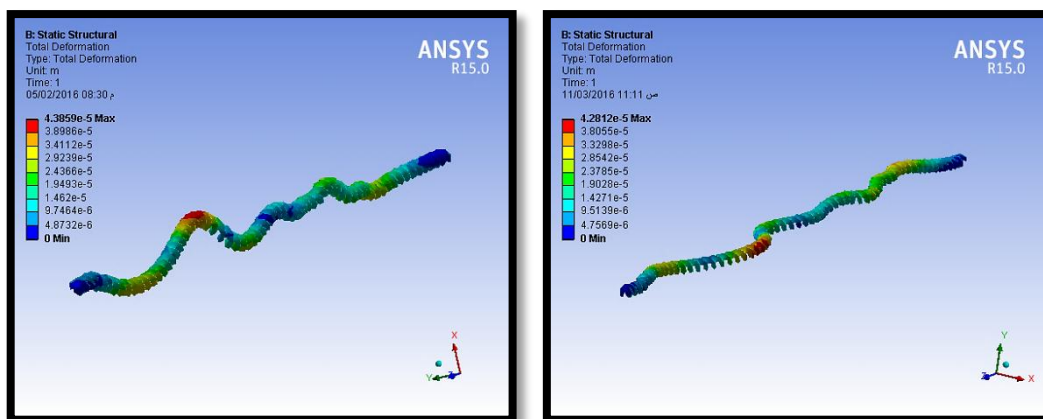
Figure 9: Total deformation from one-way interaction for (Re = 1353).



$\phi = 0 \%$

$\phi = 5 \%$

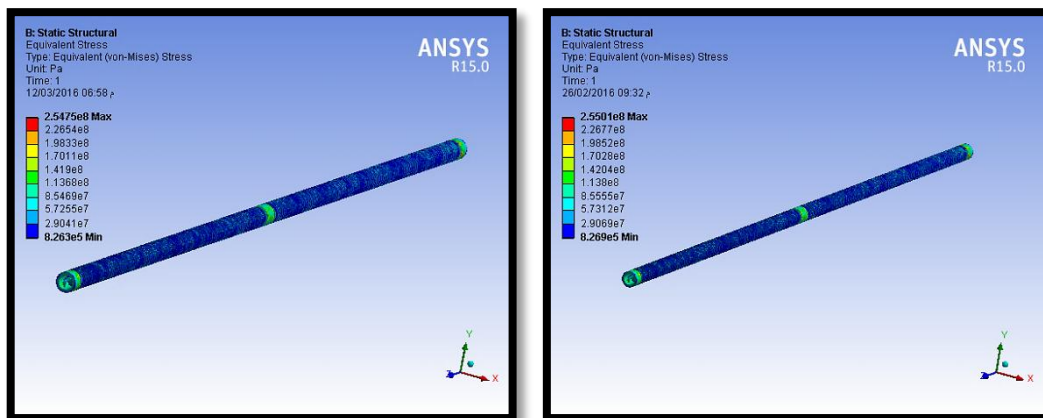
Figure 10: Total deformation from one-way interaction for (Re = 10172).



$\phi = 0 \%$

$\phi = 3 \%$

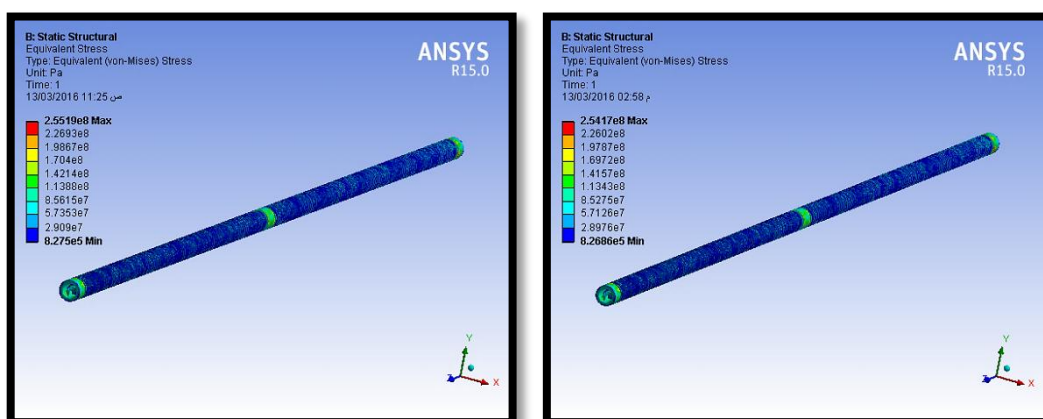
Figure 11: Total deformation for the twisted tape at ($Re = 1009$).



$\phi = 3 \%$

$\phi = 5 \%$

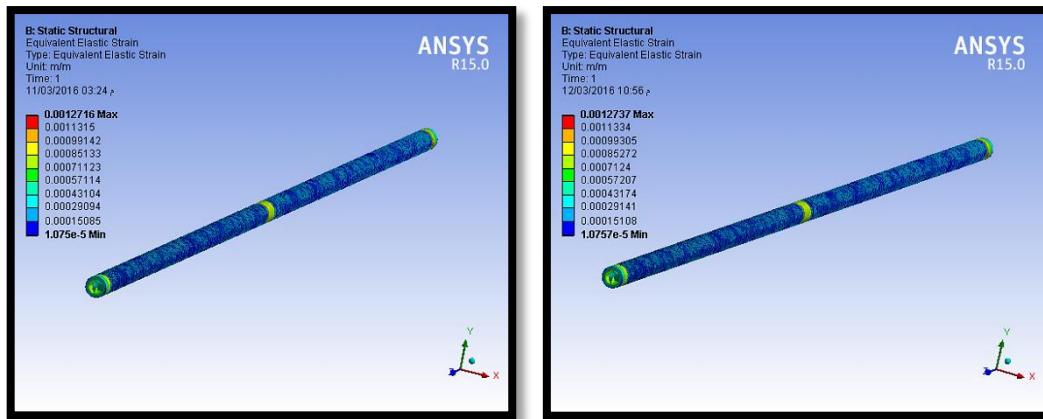
Figure 12: Stress distributions from one-way interaction for ($Re = 2033$).



$\phi = 3 \%$

$\phi = 5 \%$

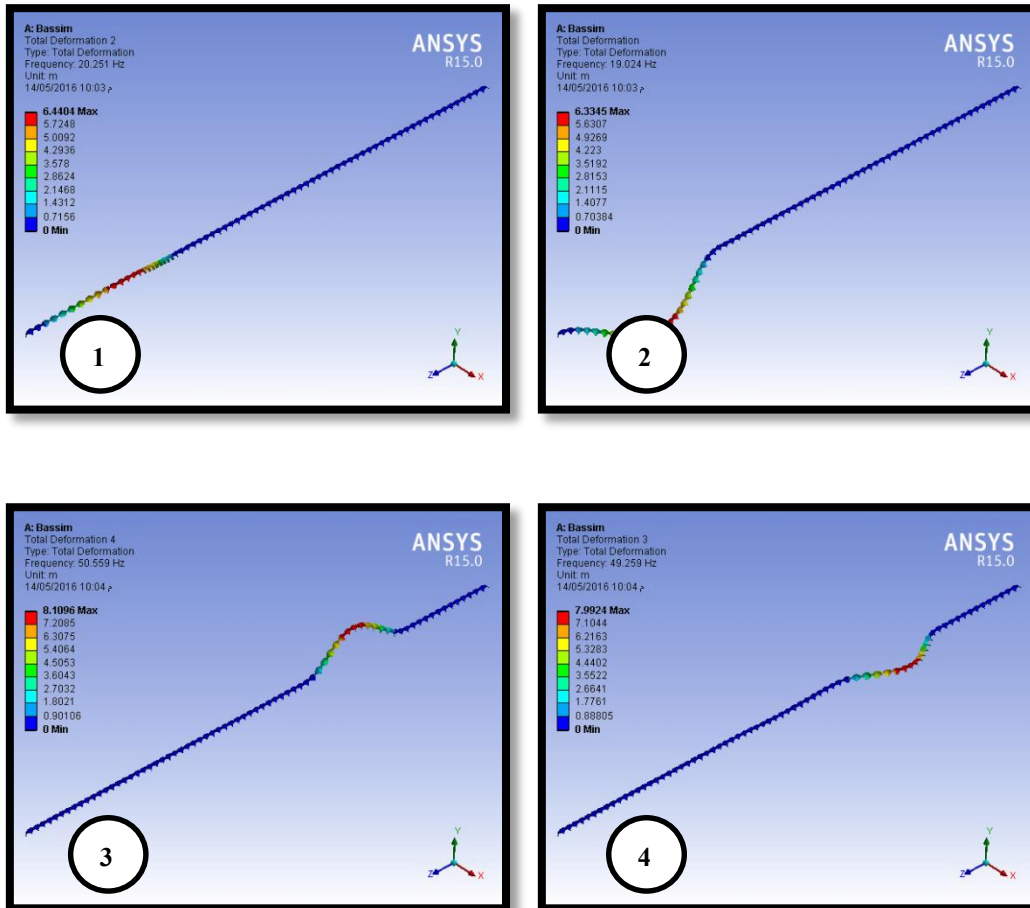
Figure 13: Stress distributions from one-way interaction for ($Re = 10172$).



Re=1354

Re=6781

Figure 14: Strain distributions from one-way interaction for ($\phi = 3\%$).



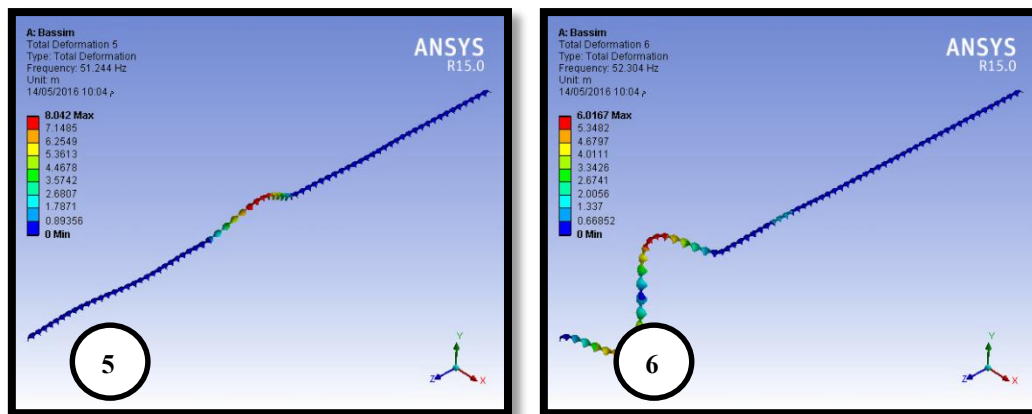


Figure 15: Six different mode shapes.

REFERENCES

- [1] Huang Y. M., Liu Y. S., Li B. H., Li Y. J. and Yue Z. F., "Natural Frequency Analysis of Fluid Conveying Pipeline with Different Boundary Condition", *Journal of Nuclear Engineering and Design*, Vol.240, pp.461-467, 2010.
- [2] Bettinali F, Molinaro P, Ciccotelli M, and Micelotta, "Transient analysis in piping networks including fluid-structure interaction and cavitation effects", *Transactions SMiRT 11*, Tokyo, Paper K35/5, 565–570.
- [3] Sreejith, B., jayaraj, K., 2004, "Finite element analysis of fluid–structure interaction in pipeline systems". *Nuclear Engineering and Design* 227, 313–322.
- [4] Hatfield FJ and Wiggert DC (1990), "Seismic pressure surges in liquid filled pipelines", *J. Pressure Vessel Technol.* 112, 279–283.
- [5] Moussou P, Vaugrante P, Guivarch M, and Seligmann D (2000), "Coupling effects in a two elbows piping system", *Proc. of 7th Int. Conf. on Flow Induced Vibrations*, Lucerne, Switzerland, 579-586.
- [6] A. S. Tissingel, A. E. Vardy and D. Fan, "Fluid Structure Interaction and Cavitation in a Single – Elbow Pipe System", *Journal of Fluids and Structures* (1996) 10, 395 – 420.
- [7] A. E. Vardy and D. Fan and A. S. Tissingel, "Fluid Structure Interaction in A T-Piece Pipe", *Journal of Fluids and Structures* (1996) 10, 763 – 786.
- [8] A. S. Tijsseling, "Water hammer with fluid–structure interaction in thick-walled pipes", *Computers and Structures* 85 (2007) 844–851.
- [9] E. Baron, Y. Berlinsky, Y. Kivity and D. Peretz "A Two-Dimensional Model for Fluid Structure Interaction in Curved Pipes", *Nuclear Engineering and Design* 80 (1984) 1-10.
- [10] Kumar, P. (2011), "A CFD Study of Heat Transfer Enhancement in Pipe Flow with Al₂O₃ Nanofluid", *World Academy of Science, Engineering and Technology* vol. 57 pp.746-750.
- [11] Versteeg, H. K., and Malalasekera, W., "An Introduction to Computational Fluid Dynamics-The Finite Volume Method", Longman group Ltd., 1995.